OPO OPHTHALMIC AND PHYSIOLOGICAL OPTICS
THE JOURNAL OF THE COLLEGE OF OPTOMETRISTS

Ophthal. Physiol. Opt. 2009 **29:** 247–255

Depolarization properties of the optic nerve head: the effect of age

Juan M. Bueno[1], Christopher J. Cookson[2], Jennifer J. Hunter[3], Marsha L. Kisilak[2,4] and Melanie C. W. Campbell[2,4,5]

[1]Laboratorio de Óptica (edificio CiOyN), Universidad de Murcia, Campus de Espinardo, 30071 Murcia, Spain, [2]Department of Physics and Astronomy, University of Waterloo, Waterloo, ON, Canada, [3]Center for Visual Science, University of Rochester, Rochester, NY, USA, [4]School of Optometry, University of Waterloo, Waterloo, ON, Canada and [5]Guelph-Waterloo Physics Institute, Waterloo, ON, Canada

Abstract

The degree of polarization (DOP) of the light reflected from the optic nerve head has been assessed by means of a polarimetric scanning laser ophthalmoscope as a function of the age of the participants. Four fundus images corresponding to independent polarization states in the recording pathway were used to compute the spatially-resolved DOP. This was not uniform across the optic nerve head and depended on both the location and the participant's age. Along a peripapillary annulus the DOP followed a double-peak pattern. Moreover, the values along this annulus decreased significantly with increasing age. This depolarization appears to originate in part in the retinal nerve fiber layer. Detailed age-dependent knowledge of the ocular depolarization properties may help to improve clinical diagnosis of the retinal nerve fiber layer.

Keywords: depolarization, fundus imaging, medical imaging, polarimetry

Introduction

Some commercially-available setups for retinal imaging are based on polarimetry and provide information to assist the diagnosis of retinal pathologies (mainly glaucoma) or the detection of amblyopia (Dreher *et al*., 1992; Greenfield *et al*., 2000; Hunter *et al*., 2003). However, all these recent technologies only give information on ocular birefringence, despite the presence of complicated additional polarization properties, including depolarization (Weale, 1966; Charman, 1980; van Blokland and van Norren, 1986; Bueno, 2001).

Ocular depolarization gives rises to partially-polarized light from incident totally-polarized light and is a property intrinsically associated with light scattering (Chipman, 1995; Bueno *et al*., 2004). The associated parameter is the degree of polarization (DOP). The term depolarization, defined as 1-DOP is also often used. In the case of the human retina, this property may be even more relevant and difficult to understand if we take into account its non-uniformity, its variation in depth and its potential change as a result of age, surgery, pathologies, or other factors.

There was an early interest in exploring the depolarizing effects of the ocular media (Brindley and Willmer, 1952; Weale, 1966), but polarimetry was not widely used until the mid-1980's (van Blokland, 1985). Although most authors studied these effects at the living human fovea (Brindley and Willmer, 1952; Weale, 1966; Charman, 1980; van Blokland, 1985; van Blokland and van Norren, 1986; Bueno, 2001, 2004), some recent studies have reported measurements of the amount of depolarization produced by the *in vitro* and *in vivo* human retinal nerve fiber layer (RNFL) (Dreher *et al*., 1992; Pelz, 1997; Twietmeyer *et al*., 2008).

Both polarized and depolarized light have been reported to improve the visibility of retinal features in images of the fundus (Bueno and Campbell, 2002; Burns *et al*., 2003; Mellem-Kairala *et al*., 2005; Miura *et al*., 2005; Bueno *et al*., 2007; Elsner *et al*., 2007).

Received: 30 October 2008
Revised form: 14 January 2009
Accepted: 19 January 2009

Correspondence and reprint requests to: Juan M. Bueno.
Tel.: +34 968 398335; Fax: +34 968 363528.
E-mail address: bueno@um.es

doi: 10.1111/j.1475-1313.2009.00644.x

The depolarization properties of light reflected from the fundus have not been fully characterized and little is known about how the different parts of the retina and the crystalline lens contribute to depolarize the light. Although the birefringent nature of the optic nerve head (ONH) is useful in clinical diagnosis, other polarization properties such as depolarization may not be negligible and may affect the performance of some retinal-imaging devices. Moreover, to our knowledge, there are no studies reporting how ocular depolarization effects are affected by age. Here, we have used a polarimetric scanning laser ophthalmoscope (SLO) to measure the DOP of the light returning from the ONH of the human eye as a function of age.

Methods

Experimental setup

Figure 1 shows a schematic diagram of the polarimetric SLO used for the measurements in this paper (Bueno and Campbell, 2002). A research SLO was modified to include an analyzer of polarization states (AU) in the image capture pathway, keeping fixed the polarization state of the incident light. Briefly, a circularly-polarized 633 nm laser beam is used for illumination. This polarization state is produced by the generator unit (GU). A rotating polygon mirror and a galvanometer are scanned in two dimensions (X and Y, respectively) to allow recording of images with a 15° field of view of the fundus (centered on the ONH for the present work). The light emerging from the eye is de-scanned through the same optics and enters the AU, which combines a rotary quarter-wave plate (RQWP) and a vertical linear polarizer (P). Finally a lens (L) focuses the beam on a confocal pinhole (AP2) and the light reaches the photomultiplier tube (PMT). For this work, a 3.3-mm entrance pupil and a confocal pinhole of 400 microns (approximately equivalent to 100 μm on the fundus) were used.

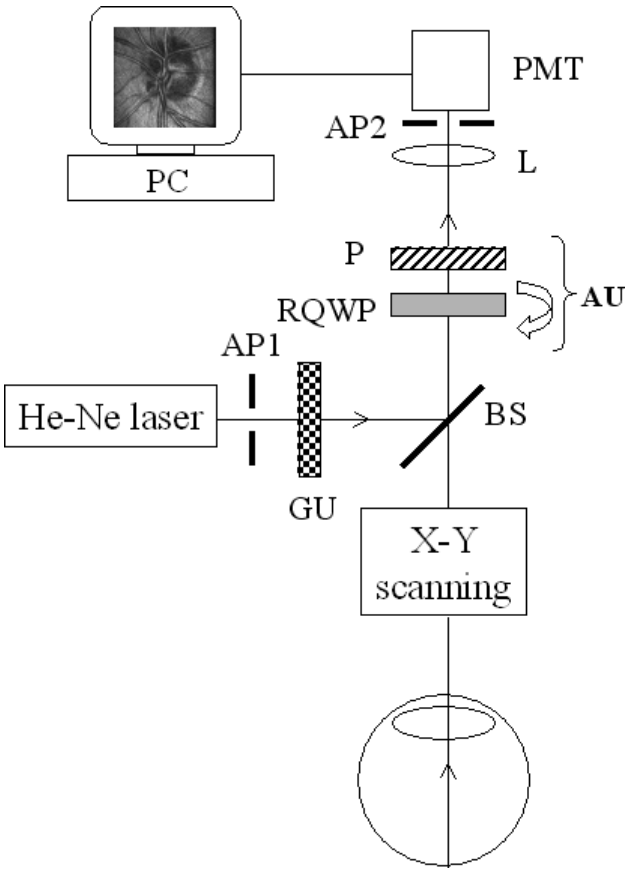

Figure 1. Schematic of the polarimetric SLO. GU and AU, generator and analyzer units; BS, beam-splitter; P, linear polarizer; RQWP, rotary quarter-wave plate; AP1 and AP2, apertures; L, positive lens; PMT, photomultiplier tube.

Participants and procedure

Eight Caucasian participants with normal vision ranging in age from 19 to 64 years, spectacle spherical refractive errors ranging from −3.5 D to +4 D and cylinder corrections < 1.5 D, were involved in the study. All participants underwent a complete ophthalmological examination to rule out the presence of any ocular pathology. A signed informed consent letter, approved by the University of Waterloo Human Ethics Committee, was obtained from all participants. The pupil was dilated with 0.5% tropicamide prior to data collection. During measurements, the participant's head was stabilized by means of a bite bar mounted on a three-axis positioning stage.

For each independent polarization state produced in the AU, a video segment at a frame rate of 28.5 Hz was recorded. These polarization states were produced by orienting the fast axis of the RQWP in the AU at four different angles. Details of this procedure can be found elsewhere (Bueno *et al.*, 2003). Noise in the images was reduced by registering and averaging 8 frames within each video segment. An image obtained without the participant in the system was chosen and averaged with additional background frames with the highest correlation to this image. This background image was subtracted from each averaged image. From the four final images (I_i, i = 1, 2, 3, 4), the elements of the Stokes vector as well as the DOP were calculated at each pixel position. For the sake of completeness, the procedure is described below.

If $(I_1, I_2, I_3, I_4)^T$ is the spatially-resolved vector containing the four registered fundus images, the spatially resolved Stokes vector, S_{OUT} is:

$$S_{OUT} = \begin{pmatrix} S_0 \\ S_1 \\ S_2 \\ S_3 \end{pmatrix} = (M_{AU})^{-1} \begin{pmatrix} I_1 \\ I_2 \\ I_3 \\ I_4 \end{pmatrix}, \quad (1)$$

with M_{AU} being an auxiliary 4×4 matrix where each row is the first row of the Mueller matrix corresponding to each independent polarization state in the AU. The first element of S_{OUT} is the actual pixel-by-pixel intensity (i.e. the image) reaching the AU and the rest of elements contain information on the polarization state of the light. Once S_{OUT} is known, the DOP can be directly calculated as (Chipman, 1995):

$$DOP = \frac{\left(S_1^2 + S_2^2 + S_3^2\right)^{1/2}}{S_0} \quad (0 \leq DOP \leq 1). \quad (2)$$

Depolarization will be referred as 1-DOP, that is, the lower the DOP is, the higher the presence of depolarization.

Anova's, Bonferroni corrected paired *t*-tests and linear regressions were used to analyze significant trends in the data.

Results

As an example, *Figure 2* shows two series of ONH images corresponding to the four polarization states produced in the AU for two different participants (29 and 64 years old respectively). The vertical line in some of the images of the older participant is an artifact from the registration operation. As expected, for each participant the quality of the four images depends on the polarization states in the AU, although this dependence seems to be stronger in the younger eye. This fact is confirmed when computing (for instance) the signal-to-noise-ratio (SNR) across the whole image. For the younger participant, highest and lowest SNR values (I_4 and I_2 images respectively) differ by 57%, however for the older participant, this difference is 5% (between the

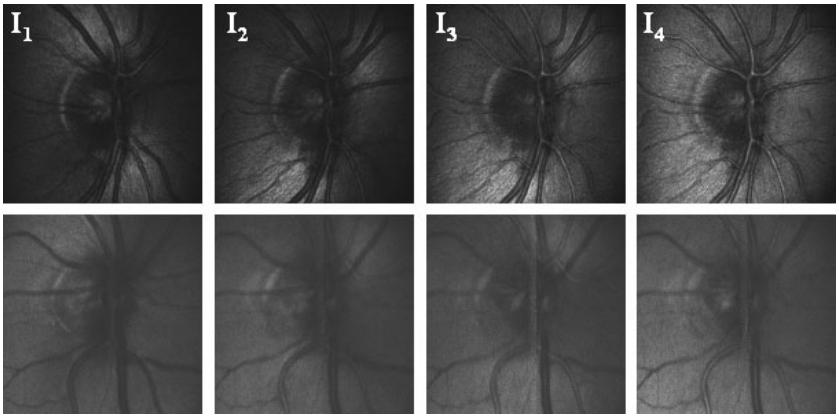

Figure 2. Polarimetric ONH images for a younger (29 year old, upper panels) and older (64 year old, bottom panels) participant corresponding to the four independent polarization states in the AU. Each image is the average of eight frames and subtends ~14°.

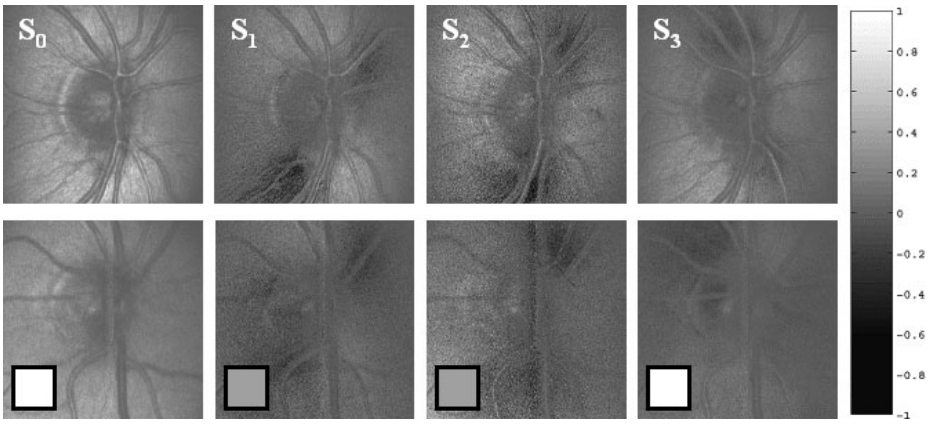

Figure 3. Spatially-resolved Stokes vector elements computed from the images of the two different participants in *Figure 2*. The grey level code is shown at the right. The insets at the bottom left of lower panels represent the elements of the vector associated with the polarization state of the incident light.

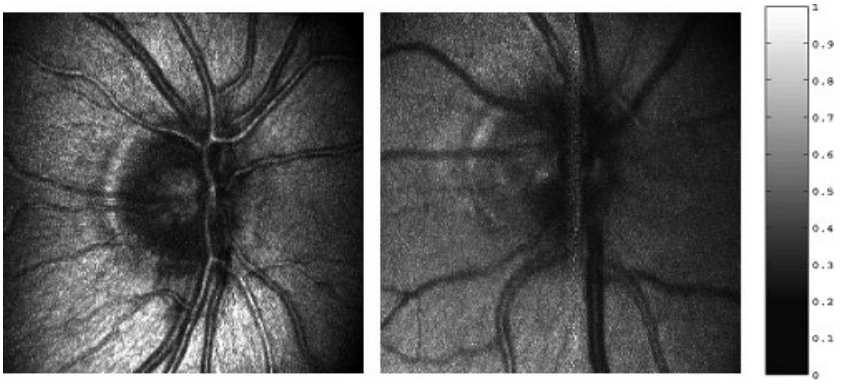

Figure 4. Spatially resolved DOP computed from the elements of the Stokes vector in *Figure 3*.

maximum and minimum SNR in the I_2 and I_4 images respectively). This influence of the AU configuration is due to the non-uniform polarization properties of the imaged retinal area, which change the polarization state of the incident light in a complicated manner (Bueno *et al.*, 2008).

The four spatially-resolved elements of the Stokes vector of the light at the AU computed from these images by means of *Equation 1*, are given in *Figure 3*. Each vector contains information on the polarimetric changes suffered by the light beam when double-passing the ocular media, being reflected at the ONH area and passing through the instrument. Differences in the data among participants will reflect differences in the participants' ocular polarization properties.

The averaged values for these Stokes elements were $(1.00, 0.40, 0.46, 0.45)^T$ and $(1.00, 0.08, 0.31, 0.14)^T$ for the younger and older participants in *Figure 3* respectively. Despite the different polarization properties for different local areas of the ONH, these averaged vectors provide some global information on the changes to the incident beam. In general, due to the presence of birefringence and depolarization, the totally-polarized incident beam is transformed into partially-polarized light.

Figure 4 shows the spatially-resolved DOP for the same participants as in *Figures 2* and *3*. The values were calculated pixel by pixel using *Equation 2*. It can be observed that the parameter varies across the image, the variations being larger in the younger eye. The averaged DOP values for the whole images were 0.36 ± 0.06 and

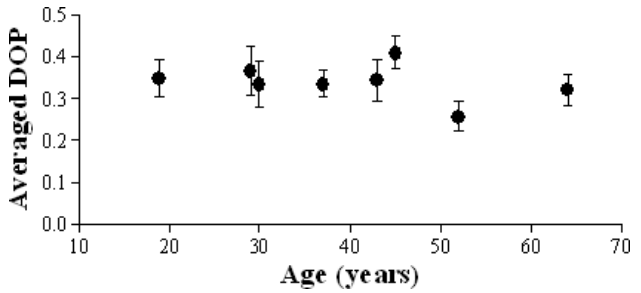

Figure 5. Mean DOP values across the entire image for all participants as a function of age. The bars represent the standard deviation of the data. There is no significant dependence on age.

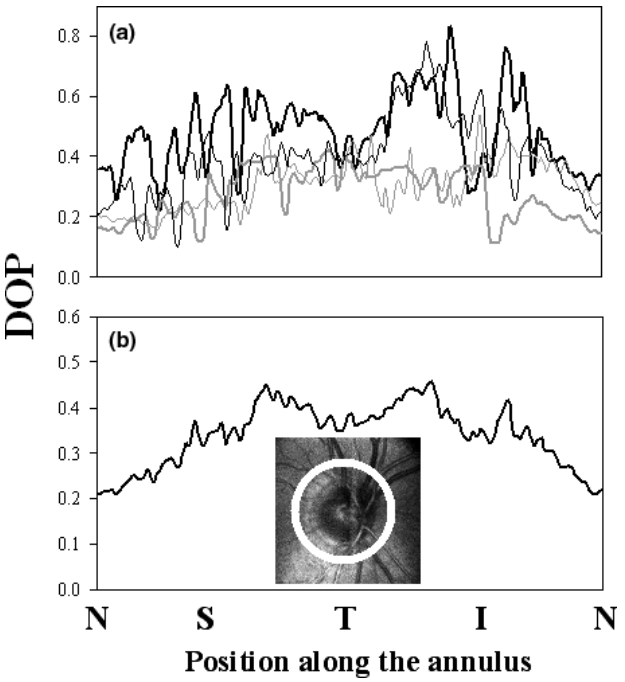

Figure 6. (a) Plot of averaged DOP values along a peripapillary annulus in 4 normal participants of different ages (black lines, young participants, 19 and 29 years old; grey lines, middle-aged and older participants, 43 and 64 years old). The superimposed white circle on the image of the ONH shows the position and size of the annulus. N, S, T and I indicate nasal, superior, temporal and inferior areas. Bonferroni corrected *t*-tests of the plotted values show significant differences between each pair of participants shown here ($p < 0.007$). An ANOVA for all participants showed a significant effect of the position on the ring ($p < 0.001$) and of age ($p < 0.001$) on the DOP values. (b) Plot of the DOP values along a peripapillary annulus averaged across all participants. Bonferroni corrected *t*-tests show that the value at 2° (N) is significantly lower than the values at the two peaks (S and I) but is not significantly different from the local (T) minimum ($p < 0.017$).

0.32 ± 0.04 for the younger and older participants respectively. *Figure 5* depicts the averaged DOP values for the entire images as a function of age. There was no significant age variation in this average ($p = 0.41$).

The DOP values in four square areas (inferior, superior and two temporal or nasal to the ONH) were calculated for five of the participants, aged 19, 29, 37, 45 and 64 years. DOP values between four of the six pairs of retinal areas differed significantly across participants ($p < 0.017$; paired *t*-test Bonferroni corrected for repeated tests). DOP values across these four areas for the 19 year-old were not significantly different from those for the 29 year-old but were significantly higher than those for the 37, 45 and 64 year-old participants (Bonferroni corrected paired *t*-tests, $p < 0.012$).

For comparison, *Figure 6a* presents for four participants of different ages (19, 29, 43 and 64 years), the DOP values along an annular region centered on the ONH with an inner radius of 3.1°and an outer radius of 3.7° (see inset). Each value along the annulus in the plot (360 angular steps) corresponds to the averaged DOP value across its width. This annulus is similar to that used to measure the peripapillary retardation for glaucoma diagnosis in commercially-available instruments (Greenfield *et al.*, 2000). Paired *t*-tests were performed on the DOP values around the annulus between participants with a Bonferroni correction for repeated tests. These results showed that there were significant differences between 24 of the 28 pairs of participants ($p < 0.007$) except for: the 19 and 30 year old; the 37 and 43 year old; the 37 and 52 year old; and the 43 and 52 year old participants.

An ANOVA analysis of all participants showed that there was a significant effect of the position on the annulus ($p < 0.001$), and age ($p < 0.001$), on the DOP values. *Figure 6b* shows the average DOP across all participants as a function of angle around the annulus. This figure shows a minimum in the nasal portion of the annulus (2°) and two peaks at 120° (superior) and 237° (inferior) with an intermediate minimum at 171° (temporal). Bonferroni paired *t*-tests of the DOP values at these locations showed that the peaks were significantly different from the nasal minimum, which was not different from the intermediate minimum ($p < 0.017$).

In *Figure 7* for the younger and older participants, some of whose data were given in *Figures 2–4*, we have plotted the DOP profile along the annulus, described together with the retardation for the same annulus. There was a significant difference between the DOP values of these participants (paired *t*-test with Bonferroni correction). For a better comparison, the retardation values have been normalized to their maximum. For both eyes, the pattern of retardation along an annulus has the typical double-peak pattern (Dreher *et al.*, 1992; Greenfield *et al.*, 2000), although this pattern is less apparent in the older participants. For each of the two participants, a linear regression of DOP to normalized retardation was significant ($p < 0.03$) but the two slopes differed in sign and the r^2 values were less than 0.05, indicating that the fits explained little of the variation in DOP.

Finally *Figure 8* depicts the averaged DOP values along the annulus around the ONH for each participant as a function of age. For these participants, an ANOVA

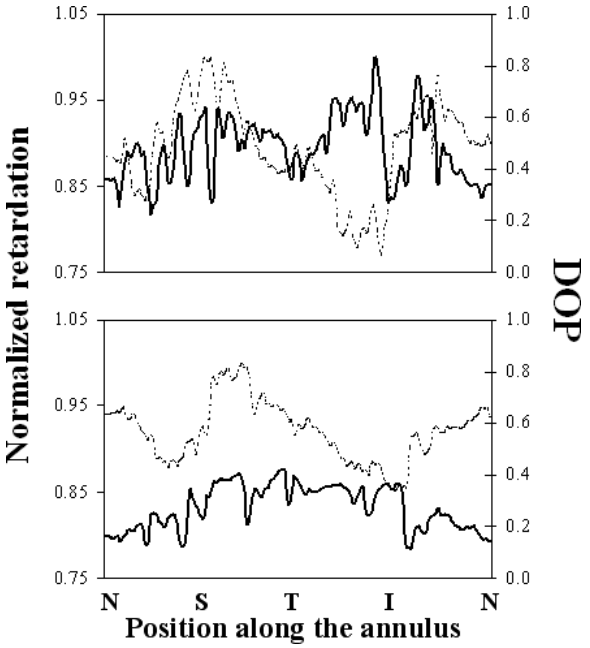

Figure 7. DOP values (solid line) and normalized retardation (dotted line) along an annulus centered in the ONH for the same two participants (29 and 64 years old) as in *Figure 2*. Paired *t*-tests on the DOP values around the annulus between these participants with a Bonferoni correction showed a significant difference between participants ($p < 0.007$). Linear regressions between DOP and retardation for each of the two participants were significant but had slopes of differing signs and explained little of the DOP variation.

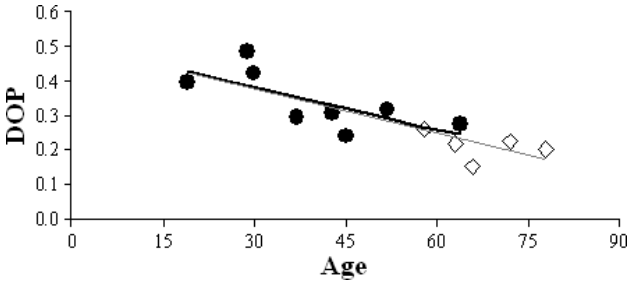

Figure 8. Averaged DOP values along the peripapillary annulus for all participants involved in this study (black circles). The black line fitted to the data gives a significant linear decrease with increasing age ($p = 0.049$). Diamonds are data from older participants replotted from Naoun *et al.* (2005). The resulting linear fit (grey line) has a $p < 0.0003$. The two linear fits are not significantly different.

showed a significant dependence on age. A linear regression showed a significant decrease of the DOP with age ($R = 0.50$, $p = 0.049$). When data from older, normal participants of Naoun *et al.* (2005) were added, the linear fit was unchanged with an improved $p < 0.0003$. Between 15 and 80 year old participants, there was an approximately 0.28 change in the average DOP value. When all values of DOP around the annulus for each of our participants were used in a univariate analysis, there was a stronger significant effect of age ($p < 0.001$).

Discussion

We have used a polarimetric SLO to analyze the effects of depolarization at the ONH in a group of normal participants with different ages. The parameter DOP, calculated pixel by pixel from the spatially-resolved Stokes vector has been used to quantify these effects. This polarization property can be computed independently from birefringence.

Some polarimetric original fundus images show details of the retinal structures that cannot be observed in the rest of the images. That is, the AU introduced in the SLO makes the quality of the registered images depend on the polarization state of this AU. This was expected, since incoming circularly total-polarized light turns into elliptically partial-polarized light after passing through the ocular optics and the retina. In addition, changes in polarization state depend on the retinal location. However, here the dependence seems to be more noticeable in younger eyes, probably because older eyes present larger levels of depolarization (scattering). Overall, the higher the depolarizing effects, the lower the effects of the AU on polarization state (Bueno, 2004). An analysis of this has been recently reported by Bueno *et al.*, (2008) and is beyond the scope of the present paper.

While most studies of the ONH and peripapillary region have concentrated on birefringence, depolarization adds important information. In normal eyes, depolarization is presumably from the retina and is affected little by corneal or retinal birefringence. Both properties modify the polarization state of the incident beam, providing a non-uniform Stokes vector associated with the emergent light. Since changes in polarization properties might change with age and be related to some pathologies, we chose to analyze the ONH, a very important location from a clinical point of view.

The average DOP across the entire image of the ONH region does not show any significant dependence with age ($p = 0.41$; *Figure 5*) perhaps because of the variation with position in the image. However, values across four areas of the image were significantly higher for the youngest participant than for the middle-aged and older participants. The age-dependence was not as strong as for the annulus around the ONH. Age is responsible for an increase of ocular scattering (i.e. depolarization), due in part to an increased scattering in the crystalline lens. This effect would be expected everywhere in the image, but we did not find this. The presence of a loosely confocal aperture in the polarimetric SLO used might be expected to reduce the contribution of scattered light originating further from the imaged structures, to depolarization.

Since measurements designed to assist the early detection of glaucoma are based on the assessment of physical changes of the retinal nerve fibers in a circular path around the ONH, we decided to study the DOP for similar areas to those used by clinical instruments. In normal eyes, the retardation changes along the annulus, with maximum values in superior and inferior bundles, and minimum values in the temporal and nasal bundles. Unlike retardation, the DOP profiles along the annulus were unique for each eye (*Figures 6 and 7*), and did not appear to follow as pronounced a pattern. However, there was significant dependence of DOP on position on the annulus. In addition, there was a significant dependence of the DOP profile on age. When the DOP was averaged along the annulus, these values decreased with a significant linear dependence on increasing age (*Figure 8*). Linear regression suggests a decrease of 63% in the average DOP around this annulus between 15 and 80 years of age. Since depolarization is usually associated with the presence of scattering (Bueno *et al.*, 2004), this decrease in DOP might indicate that older eyes present higher levels of retinal scattering, at least within the analyzed area of the RNFL.

The analysis of the DOP in the human eye has been a topic of interest to several authors. van Blokland was the first to use a (non-imaging) polarimeter to study the DOP of the light emerging from the living human eye (van Blokland, 1985; van Blokland and van Norren, 1986). For wavelengths of 488, 514 and 568 nm and a $\sim 2°$ retinal field centered on the fovea, the DOP of the light passing the central pupil was ~ 0.75, but it decreased down to ~ 0.40 for 647 nm. At peripheral retinal sites (5° and 8° temporal) lower DOP values were observed (approximately a 5% reduction). Moreover, they also reported that the DOP was almost invariant with the angle and position of the incident beam on the pupil, the bleaching level and the retinal region. In young normal eyes, 633-nm double-pass retinal images of the point-spread function centered at the fovea showed DOP values of 0.83, which decreased to 0.25 in the outer area of the image (Bueno, 2001). For extended retinal areas and using 780 nm polarimetric SLOs, averaged DOP values ranging from 0.71 to 0.86 have been reported (Pelz, 1997; Twietmeyer *et al.*, 2008).

In order to study *in vitro* human retinas, Dreher *et al.* (1992) used a 633 nm scanning laser polarimeter. The DOP varied between 0.5 and 0.87 within a ring around the ONH. DOP values for our younger participants fall within this range while values for older participants are lower.

Using a modified biomicroscope, Naoun *et al.* (2005) evaluated the DOP at four retinal locations (inferior, superior, nasal and temporal) around the ONH in a set of 10 participants (5 normal, aged 58–78 and 5 glaucomatous). DOP values ranged between 0.09 and 0.32 for normal eyes, and between 0.02 and 0.15 for glaucomatous eyes. For the analyzed areas, the DOP values for glaucomatous eyes were lower than those found in normal eyes. Within each normal participant, the DOP values for temporal and nasal locations were clearly lower than those obtained at superior and inferior areas. This behavior was similar to that found for the RNFL thickness by means of OCT techniques. For the glaucomatous population this was not observed, which was thought to be due to the loss of retinal fibers.

Our measurements around the ONH also show a significant dependence of DOP on position (*Figure 6*). Nasal DOP values were significantly lower than superior and inferior peaks and not significantly different from the lower temporal value. The relationship between the retinal nerve fiber thickness and the amount of depolarization is not simple. The DOP values shown in this work ranged between 0.10 and 0.82. These are similar to those values reported for other retinal areas (Bueno and Vohnsen, 2005) and they lie in the upper range of the values reported by Naoun *et al.* (2005). Most participants involved in the present study were younger than those involved in Naoun *et al.*'s experiment. For our one participant older than 54 years, the DOP ranged between 0.11 and 0.42, similar to their values reported for normal participants. We then added their normal participant values to *Figure 8*. The combined data were fitted with a straight line which was not significantly different from the fit to our data. The resulting linear fit,

$$DOP = 0.5097 - 0.0043 \cdot (age), \tag{3}$$

has an r^2 of 0.71, implying that age accounts for a large amount of the variation in the data.

The localization of both the retinal reflection and the sources of retinal depolarization have been a topic of interest for different authors (see for instance (Bueno, 2001) and references therein). Most reported that the light retaining polarization and the depolarized portion came from different retinal layers, but they did not agree in identifying these layers. Since polarization-sensitive optical coherence tomography (PS-OCT) was first reported (Hee *et al.*, 1992) the available information on depth-dependent polarization retinal imaging has increased. In particular, PS-OCT has been recently used to explore depolarization in ocular structures (Pircher *et al.*, 2006). Depolarizing tissues are associated with random retardation and azimuth values (also called polarization scrambling) and the retinal pigment epithelium (RPE) has been identified as the retinal depolarizing layer. Since the RPE is readily visualized, this technique has been used successfully in participants with differing retinal pathologies to identify, e.g., detachments, atrophies, thickening and absence of RPE (Pircher *et al.*, 2006; Götzinger *et al.*, 2008; Michels *et al.*, 2008).

In a healthy retina, the different layers are supposed to be well-ordered, which implies that the depolarization effects should be weak. However, when the retina presents some pathology the structure becomes less ordered, and the scattering levels increase, as do the effects of retinal depolarization. This fact has been used by Elsner, Burns and co-workers to explore participants with different ocular pathologies (age-related macular degeneration, hyperpigmentation, chorioretinopathy). Depolarization maps were reported to improve the contrast visibility of subretinal features and affected areas were better visualized (Burns *et al.*, 2003; Mellem-Kairala *et al.*, 2005; Miura *et al.*, 2005). In particular this non-invasive polarization-sensitive imaging is able to localize hyperpigmented areas, and retinal regions containing drusen and exudation, with increased contrast. These features were often barely visible with conventional retinal imaging.

Our results show a substantial, significant increase in depolarization of light returning from the retina with increasing age in normal participants (i.e. DOP values decrease). The sources of this depolarization could include the crystalline lens, which increasingly depolarizes light with increasing age (Bueno and Campbell, 2003), and the retina. An increase in retinal scattering, could result from changes in retinal structures with aging, in particular, changes in the RNFL. The similarity of data from our setup with a loosely confocal aperture and those from a biomicroscope is suggestive of depolarization effects close to the in-focus retinal plane. The DOP variation along an annulus also supports a source of depolarization within the RNFL. Further work comparing the normal eyes in this study with eyes with pathologies might help us better understand the sources of ocular depolarization. The resulting age dependence of DOP could reduce the utility of depolarization maps in older participants in whom other polarization imaging methods may have utility (Bueno and Campbell, 2002; Bueno *et al.*, 2007).

The polarization information within either the Mueller matrix or the Stokes vector is often not easy to extract. In particular, DOP affects the analysis of retardation from polarisation measurements. That is,

when computing the retardation associated with birefringent structures, the information on depolarization must be taken into account, otherwise results on retardation might be misleading (Bueno, 2004). To our knowledge, commercially-available instruments designed to compute the RNFL thickness from measured retardation values do not take this fact into account (Knighton and Huang, 2002; Burns *et al.*, 2003). These devices use a configuration of linear polarizers, and the minimum intensity light for the crossed channel is considered as depolarized light. A configuration involving only linear polarizers cannot yield the actual DOP value, since the circular component cannot be computed. In this sense, a more accurate computation of the ocular retardation could be made using the age and position dependence of the DOP derived here.

In conclusion, SLO imaging polarimetry has been used to extract the DOP of the ONH for a set of participants of different ages. The parameter depended on both the imaged position and the participant's age. Since all eyes had transparent media (i.e. depolarizing effects were weak) and DOP varied with retinal position, the RNFL may contribute most to depolarization. For an annulus around the ONH, the mean DOP was found to decrease significantly with age. The DOP dependence on age and position derived here may improve the accuracy of RNFL thickness measurements. An understanding of the DOP changes with age may lead to a better understanding of age changes in the RNFL.

Acknowledgements

This work was supported by NSERC (Canada) and grant FIS2007-64765 from the Ministerio de Educatión y Ciencia (Spain).

References

van Blokland, G. J. (1985) Ellipsometry of the human retina in vivo: preservation of polarization. *J. Opt. Soc. Am. A* **2,** 72–75.

van Blokland, G. J. and van Norren, D. (1986) Intensity and polarization of light scattered at small angles from the human fovea. *Vision Res.* **26,** 485–494.

Brindley, G. S. and Willmer, E. N. (1952) The reflexion of light from the macular and peripheral fundus oculi in man. *J. Physiol.* **116,** 350–356.

Bueno, J. M. (2001) Depolarization effects in the human eye. *Vision Res.* **41,** 2687–2696.

Bueno, J. M. (2004) The influence of depolarization and corneal birefringence on ocular polarization. *J. Opt. A: Pure Appl. Opt.* **6,** S91–S99.

Bueno, J. M. and Campbell, M. C. W. (2002) Confocal scanning laser ophthalmoscopy improvement by use of Mueller-matrix polarimetry. *Opt. Lett.* **27,** 830–832.

Bueno, J. M. and Campbell, M. C. W. (2003) Polarization properties for *in vitro* old human crystalline lens. *Ophthal. Physiol. Opt.* **23,** 109–118.

Bueno, J. M. and Vohnsen, B. (2005) Polarimetric high-resolution confocal scanning laser ophthalmoscope. *Vision Res.* **45,** 3526–3534.

Bueno, J. M., Berrio, E. and Artal, P. (2003) Aberro-polariscope for the human eye. *Opt. Lett.* **28,** 1209–1211.

Bueno, J. M., Berrio, E., Ozolinsh, M. and Artal, P. (2004) Degree of polarization as an objective method of estimating scattering. *J. Opt. Soc. Am. A* **21,** 1316–1321.

Bueno, J. M., Hunter, J. J., Cookson, C. J., Kisilak, M. L. and Campbell, M. C. W. (2007) Improved scanning laser fundus imaging using polarimetry. *J. Opt. Soc. Am. A* **24,** 1337–1348.

Bueno, J. M., Cookson, C. J., Hunter, J. J., Kisilak, M. L. and Campbell, M. C. W. (2008) 'Imaging the fundus of theeye through polarization: dependence with age,' 2008 Annual Meeting Abstract and Program Planner, http://www.arvo.org, abstract #3209.

Burns, S. A., Elsner, A. E., Mellem-Kairala, M. B. and Simmons, R. B. (2003) Improved contrast of subretinal structures using polarization analysis. *Invest. Ophthalmol. Vis. Sci.* **44,** 4061–4068.

Charman, W. N. (1980) Reflection of plane-polarized light by the retina. *Br. J. Physiol. Opt.* **34,** 34–49.

Chipman, R. A. (1995) Polarimetry. In: *Handbook of Optics* (ed. M. Bass), Vol. 2, 2nd edn. McGraw-Hill, New York, Chapter 22.

Dreher, A. W., Reiter, K. and Weinreb, R. N. (1992) Spatially resolved birefringence of the retinal never fiber layer assessed with a retinal laser ellipsometer. *Appl. Opt.* **31,** 3730–3735.

Elsner, A. E., Weber, A., Cheney, M. C., VanNasdale, D. A. and Miura, M. (2007) Imaging polarimetry in patients with neovascular age-related macular degeneration. *J. Opt. Soc. Am. A* **24,** 1468–1480.

Götzinger, E., Pircher, M., Geitzenauer, W., Ahlers, C., Baumann, B., Michels, S., Schmidt-Erfurth, U. and Hitzenberger, C. K. (2008) Retinal pigment epithelium segmentation by polarization sensitive optical coherence tomography. *Opt. Express* **16,** 16410–16422.

Greenfield, D. S., Knighton, R. W. and Huang, X.-R. (2000) Effect of corneal polarization axis on assessment of retinal nerve fiber layer thickness by scanning laser polarimetry. *Am. J. Ophthalmol.* **129,** 715–722.

Hee, M. R., Huang, D., Swanson, E. A. and Fujimoto, J. G. (1992) Polarization sensitive low coherence reflectometer for. birefringence characterization and ranging. *J. Opt. Soc. Am. B* **9,** 903–908.

Hunter, D. G., Shah, A. S., Sau, S., Nassif, D. and Guyton, D. L. (2003) Automated detection of ocular alignment with biocular retinal birefringence scanning. *Appl. Opt.* **42,** 3047–3053.

Knighton, R. W. and Huang, X. R. (2002) Analytical methods for scanning laser polarimetry. *Opt.* Express. **10,** 1179–1189.

Mellem-Kairala, M. B., Elsner, A. E., Weber, A., Simmons, R. B. and Burns, S. A. (2005) Improved contrast of peripap-

illary hyperpigmentation using polarization analysis. *Invest. Ophthalmol. Vis. Sci.* **46,** 1099–1106.

Michels, S., Pircher, M., Geitzenauer, W., Simader, C., Götzinger, E., Findl, O., Schmidt-Erfurth, U. and Hitzenberger, C. K. (2008) Value of polarisation-sensitive optical coherence tomography in diseases affecting the retinal pigment epithelium. *Br. J. Ophthalmol.* **92,** 204–209.

Miura, M., Elsner, A. E., Weber, A., Cheney, M. C., Oshako, M., Usui, M. and Iwasaki, T. (2005) Imaging polarimetry in central serous chorioretinopathy. *Am. J. Ophthalmol.* **140,** 1014–1019.

Naoun, O. K., Louis-Dorr, V., Allé, P., Sablon, J. C. and Benoit, A. M. (2005) Exploration of the retinal nerver fiber layer thickness by measurement of the linear dichroism. *Appl. Opt.* **44,** 7074–7082.

Pelz, B. C. E. (1997) Entwicklung eines elektrooptischen Ellipsometers zur *in vivo* Evaluation der retinalen Nervenfaserschicht und der Hornhaut des menschlichen Auges. Ph D Thesis, Universität Heidelberg, Germany.

Pircher, M., Götzinger, E., Findl, O., Michels, S., Geitzenauer, W., Leydolt, C., Schmidt-Erfurth, U. and Hitzenberger, C. K. (2006) Human macula investigated in vivo with polarization-sensitive optical coherence tomography. *Invest. Ophthalmol. Vis. Sci.* **47,** 5487–5494.

Twietmeyer, K. M., Chipman, R. A., Elsner, A. E., Zhao, Y. and VanNasdale, D. (2008) Mueller matrix retinal imager with optimized polarization conditions. *Opt. Express* **16,** 21339–21354.

Weale, R. A. (1966) Polarized light and the human fundus oculi. *J. Physiol.* **186,** 925–930.